Coherent excitation of a two-state system by a train of short pulses

Nikolay V. Vitanov and Peter L. Knight
Optics Section, Blackett Laboratory, Imperial College, Prince Consort Road, London SW7 2BZ, United Kingdom
(Received 28 December 1994)

A theoretical nonperturbative study of the coherent excitation of a two-state system by N consecutive equally spaced identical pulses is presented. General relations between the evolution matrix elements in the cases of one and N pulses are obtained in a closed form. For pulse envelopes allowing analytical solutions, these relations enable analytical treatment of pulse-train excitation; for pulses that can only be treated numerically, they shorten the computations by a factor of N. The relations show that the multiple-pulse excitation of a two-state system can be considered as a quantum analog of the diffraction grating. The interaction dynamics substantially depends on the way the train is produced because the phase shift that is accumulated by the probability amplitudes due to the free evolution of the system during and between the pulses differs. In the limit of weak excitation, the results recover earlier conclusions based on perturbative treatments. Simple formulas are derived for the conditions for complete population inversion (CPI) and complete population return (CPR), which differ from the single-pulse ones. These general results are applied to four particular cases that allow analytical solutions: resonant, rectangular, Rosen-Zener, and Allen-Eberly pulses. A common feature in all these cases is that the number and the amplitude of oscillations in the state populations increase with the number of pulses, while their width decreases. For rectangular pulses, CPI is possible below a given value of the ratio between the detuning and the pulse area; this value increases nearly linearly with the number of pulses. For the Rosen-Zener model, CPI is found to be possible for two and more pulses, while it is impossible for a single nonresonant pulse. It is shown that for a given number of pulses there is an upper limit on the detuning for which CPI can be observed; this limit increases logarithmically with the number of pulses. For the Allen-Eberly model, CPR is established to be possible for more than one pulse, while it is impossible for a single pulse. The cases of even and odd number of pulses are shown to lead to substantially different results. The limitations imposed on the detuning by the conditions for CPR and CPI are derived and discussed.

PACS number(s): 42.50.Hz, 32.80.Bx, 33.80.Be

I. INTRODUCTION

Many processes in optics, magnetic resonance, and slow atomic collisions can be considered as involving only two states. Despite its simplicity, the two-state approximation provides a useful and frequently realistic description of these processes. Detailed discussions and extensive reference lists devoted to the two-state problem can be found in Refs. [1–4]. To be specific, we will use the optical terminology, relating the system to an atom, the field to a laser pulse, and the interaction to excitation, although most of the results are valid in general.

In contrast to the numerous publications concerning interaction of a two-state system with a single pulse there are only a limited number of studies of atomic excitation by pulse trains. In terms of applications, pulse-train excitation provides a route to high-resolution spectroscopy exploiting interference to generate narrow lines. In this connection, we should mention the work devoted to the observation of Ramsey fringes [5] in the optical domain [6–13]. Bergquist, Lee, and Hall [6] have observed Ramsey fringes in the saturated-absorption signal from Ne* atoms crossing three and four equally spaced spatially separated standing-wave laser beams. A variant of this method has been implemented by Chebotayev and coworkers [7]. Ramsey fringes have also been observed by Doppler-free two-photon spectroscopy [8–11]. Baklanov, Chebotayev, and Dubetsky [8] have used two spatially separated interaction zones while in the experiments of Salour [9,10] the atoms have interacted with two time-delayed phase-coherent laser pulses. Hänsch and co-workers [11] have utilized a train of phase-coherent pulses produced by multiple reflections of a single pulse injected into an optical resonator. Pulse trains have been used for high-resolution spectroscopy by other authors as well [12]. Optical Ramsey fringes induced by a train of Gaussian pulses have been analyzed theoretically by Thomas [13]. In these studies, the pulse intensity has been small and the theoretical results have been derived by perturbative methods [6–11] and by the first-order Magnus approximation [13]. Recently, excitation by a train of intense laser pulses has been treated by several authors in the case of a general two-level atom [14,15] and in the case of mesospheric sodium in connection with its use as a synthetic beacon in adaptive optics [15–19]. In these studies relaxation has been accounted for and the response of the atom has mainly been calculated numerically either by matrix multiplication of the single-pulse solution [14,17] or by direct numerical integration of the optical Bloch equations [15,16]. Analytically, basic attention has been paid to the steady-state solution of the Bloch equations [14–16,18,19]. Pulse

shapes have included rectangular [14], Gaussian [15–18], and general [15,18]. In Refs. [14–18], the detuning has been assumed constant while Peterson and Gavrielides [19] have discussed the steady-state solution for chirped pulses. The power spectrum of the light scattered by a two-level atom in the presence of a pulse-train driving field has been analyzed by Newbold and Salamo [20]. Furthermore, theoretical treatment of multiple-pulse excitation of three-level systems has been carried out by Knight and co-workers [21]. Experimentally, Ramsey fringes with three-level sodium atoms have been observed, e.g., by Thomas *et al.* [22]. Pulse-train excitation of multilevel systems has been studied by Greenland [23], who has applied the precise Magnus solution to a train of delta-function pulses, and by Thomas [24] who has treated perturbatively the case of Gaussian pulses.

In the present work we develop a general analytical description of coherent excitation of a two-state system by a set of N consecutive equally spaced identical pulses. The formalism allows us to describe multiple-pulse excitation given the single-pulse solutions. In what follows we will assume that relaxation effects are not present or can be neglected. On the one hand, this restricts the applicability of our results to the case of short pulses and high repetition rates compared with the relaxation times of the system. In fact, this is not an overly restrictive limitation regarding the recent advances in laser technology [25] and the existence of dipole-allowed transitions with relatively long relaxation times in some atoms [26]. On the other hand, the absence of relaxation means that the excitation is coherent, which leads to interesting interference features in the transition probability. It also admits analytical treatment of pulses of smooth shape and nonzero constant or chirped [27] detuning. This is particularly attractive regarding the recent advances in pulse shaping [28].

The paper is organized as follows. In Sec. II, we present the general closed-form relations between the elements of the evolution matrix for interaction with N pulses and the elements of the single-pulse evolution matrix. These relations allow us to utilize the existing single-pulse analytical solutions to the two-state problem in the general case of N pulses. The evolution matrix treatment is very convenient because the matrix contains information about the interaction only but not about the initial conditions; hence, the pulse-train evolution matrix can be obtained by matrix multiplication of the single-pulse one provided the pulses are identical, equally spaced, and nonoverlapping, which will be assumed in what follows. The remarkably simple closed-form expressions are derived in the Appendix. In Sec. II E, we discuss the general properties of the transition probability. In Sec. II F, we present the conditions for complete population inversion and return, which in general differ from those for a single pulse. In Secs. III and IV, we consider multiple-pulse excitation in the cases of exact resonance and rectangular pulses. In Secs. V and VI, we treat the application of our results to two more sophisticated and physically distinct cases: Rosen-Zener [29] and Allen-Eberly [1] pulses. The rectangular and the Rosen-Zener pulses involve constant detuning, which means the transitions are nonadiabatic while in the Allen-Eberly model the pulses are chirped, the transitions being of adiabatic nature. As for single pulses, the two cases lead to considerably different results for N pulses. It should be noted that the Rosen-Zener and the Allen-Eberly pulses can be treated together as shown by Demkov and Kunike [30] and later by Hioe [31] in the case of a single pulse. However, it is more instructive to consider them separately as they represent different physical situations. It is also interesting to compare the rectangular and the Rosen-Zener pulses: although both represent excitation by symmetric pulses of constant detuning they have rather different envelope shapes, the Rosen-Zener pulse being smooth and hence, much more adiabatic. This fact makes the transition probabilities quite different for single pulses and consequently, for pulse trains. Finally, in Sec. VII we summarize our results.

II. EVOLUTION-MATRIX DESCRIPTION OF PULSE-TRAIN EXCITATION

A. The atom

When relaxation is not present or can be neglected, the time evolution of a two-state quantum system is governed by the Schrödinger equation

$$i\hbar\frac{\partial\psi}{\partial t}=H\psi \ . \tag{1}$$

We will work in the interaction representation in which the wave function of the two-state system is given by

$$\psi=C_1(t)e^{-i\omega_1 t}|1\rangle+C_2(t)e^{-i\omega_2 t}|2\rangle \ , \tag{2}$$

where $C_1(t)$ and $C_2(t)$ are the probability amplitudes of states $|1\rangle$ and $|2\rangle$ while $\hbar\omega_1$ and $\hbar\omega_2$ are their energies. The atomic transition frequency is given by $\omega_a=\omega_2-\omega_1$ ($\omega_2>\omega_1$). The Hamiltonian has the form $H(t)=H_0+V(t)$, where H_0 is the unperturbed Hamiltonian in the absence of external fields, that is, $H_0|k\rangle=\hbar\omega_k|k\rangle$ ($k=1,2$). The operator $V(t)$ describes the interaction of the atom with the pulse train, which in the electric-dipole approximation is given by $V(t)=-\mathbf{d}\cdot\mathbf{E}(t)$ where $\mathbf{d}$ is the transition dipole moment operator and $\mathbf{E}(t)$ is the electric field of the train. For electric-dipole–induced transitions among bound states of an isolated atom the matrix representation $V_{mn}(t)$ of $V(t)$ in the basis of the states $|1\rangle$ and $|2\rangle$ usually has no diagonal elements [2], i.e., $V_{11}=V_{22}=0$, which will be assumed in what follows.

B. The field

The electric field $\mathbf{E}(t)$ of the train of N equally spaced identical pulses depends on the way the pulse train is produced. When the individual pulses are not frequency-swept (chirped) two possible forms of the field are

$$\mathbf{E}(t)=\mathrm{Re}\sum_{k=0}^{N-1}\mathbf{e}E_0(t-kT)e^{i\omega t+i\phi} \quad (\omega=\text{const}) \ , \tag{3a}$$

$$\mathbf{E}(t)=\mathrm{Re}\sum_{k=0}^{N-1}\mathbf{e}E_0(t-kT)e^{i\omega t-ik\omega T+i\phi} \quad (\omega=\text{const}) \ . \tag{3b}$$

The unit vector $\mathbf{e}$, which is generally complex, defines the polarization direction. We will assume that the field phase ϕ is constant; then it does not influence the interaction dynamics and without loss of generality will be set equal to zero. $E_0(t-kT)$ describes the slowly varying (on the scale of the carrier laser frequency ω) electric field amplitude of the kth pulse and T is the repetition time (the period) of the pulse train. Field (3a) corresponds to a train of pulses that are portions of the same sinusoid, e.g., a train produced by pulsed lasers [14–19] or by pulsed amplification of a cw laser wave [9,10]. Field (3b) describes, for example, a sequence of phase-locked pulses produced by the same laser pulse [9–11,13], e.g. in an optical delay line [9,10] or by injecting a single pulse into an optical cavity formed by two mirrors [11] with high reflectivities.

Both fields (3a) and (3b) correspond to $\omega=$const. To allow the pulses to be frequency-swept (chirped), instead of ωt we introduce the function $\zeta_k(t)$ defined by

$$\zeta_k(t)=\int_0^t \omega(t'-kT)dt' .$$

The electric field is

$$\mathbf{E}(t)=\mathrm{Re}\sum_{k=0}^{N-1}\mathbf{e}E_0(t-kT)e^{i\zeta_k(t)} , \tag{4a}$$

$$\mathbf{E}(t)=\mathrm{Re}\sum_{k=0}^{N-1}\mathbf{e}E_0(t-kT)e^{i[\zeta_k(t)-\zeta_k(kT)]} . \tag{4b}$$

and it generalizes Eqs. (3a) and (3b), respectively. Chirped are the Allen-Eberly pulses [1], which will be considered in Sec. VI.

For field (4a) the atom-field coupling $V_{12}(t)$ is given by (see Ref. [2], Sec. 3.3)

$$V_{12}(t)=\hbar\sum_{k=0}^{N-1}\Omega(t-kT)\cos\zeta_k(t)$$

for a linear polarization , (5)

$$V_{12}(t)=\tfrac{1}{2}\hbar\sum_{k=0}^{N-1}\Omega(t-kT)e^{i\zeta_k(t)}$$

for a circular polarization , (6)

where $\Omega(t)=|\mathbf{d}\cdot\mathbf{e}|E_0(t)/\hbar$ is the single-pulse Rabi frequency, $\Omega(t-kT)$ being the envelope of the kth pulse. For field (4b), $\zeta_k(t)$ should be replaced by $\zeta_k(t)-\zeta_k(kT)$ in Eqs. (5) and (6).

C. The equations

With the interaction (5) or (6) the Schrödinger equation (1) transforms into two coupled equations for the probability amplitudes

$$\begin{aligned} i\frac{dC_1(t)}{dt}&=\tfrac{1}{2}\sum_{k=0}^{N-1}\Omega(t-kT)e^{-i\Lambda_k(t)}C_2(t) ,\\ i\frac{dC_2(t)}{dt}&=\tfrac{1}{2}\sum_{k=0}^{N-1}\Omega(t-kT)e^{+i\Lambda_k(t)}C_1(t) , \end{aligned} \tag{7}$$

where

$$\Lambda_k(t)=\int_0^t\Delta(t'-kT)dt' \tag{8}$$

and $\Delta(t)=\omega_a-\omega(t)$ is the atom-field detuning. For an interaction corresponding to the electric field (4b) the equations are similar to Eqs. (7) with $\Lambda_k(t)$ replaced by $\Lambda_k(t)-\Lambda_k(kT)+k\omega_a T$. To arrive at Eqs. (7) in the case of linearly polarized light (5) in optics, the rotating-wave approximation [1,2] is invoked. We will impose the standard initial conditions

$$C_1(t\to-\infty)=1,\quad C_2(t\to-\infty)=0 , \tag{9}$$

which imply the system is initially in state $|1\rangle$. The problem is to find the probability amplitudes $C_1(t)$ and $C_2(t)$ provided $\Omega(t)$ and $\Delta(t)$ are known. In the case of coherent pulsed excitation, of particular interest are the values of $C_1(t)$ and $C_2(t)$ at $t\to+\infty$, i.e., after the pulses have turned off.

D. The evolution matrix

It is convenient to study the interaction of a system with N consecutive equally spaced identical pulses in terms of the evolution matrix $\mathbf{S}$, which is a 2×2 complex matrix defined by

$$\mathbf{C}(+\infty)=\mathbf{S}\mathbf{C}(-\infty) , \tag{10}$$

where $\mathbf{C}(t)=(C_1(t),C_2(t))^T$. The supposed absence of relaxation effects leads to the probability conservation at any time: $|C_1(t)|^2+|C_2(t)|^2=1$. This condition implies that the evolution matrix is unitary, i.e., $\mathbf{S}^\dagger=\mathbf{S}^{-1}$ and its determinant is equal in modulus to 1. The fact that in the absence of interaction the probability amplitudes do not change [which is the case in the interaction representation (2)] imposes the choice $\det\mathbf{S}=1$. Then it can be shown that $S_{11}=S_{22}^*$, $S_{12}=-S_{21}^*$, and hence, for a single pulse, the $\mathbf{S}$ matrix can be parametrized as follows

$$\mathbf{S}_1=\begin{bmatrix} a_1+ib_1 & c_1+id_1\\ -c_1+id_1 & a_1-ib_1\end{bmatrix}$$

$$(a_1^2+b_1^2+c_1^2+d_1^2=1) \tag{11}$$

and in a similar way for N pulses

$$\mathbf{S}_N=\begin{bmatrix} a_N+ib_N & c_N+id_N\\ -c_N+id_N & a_N-ib_N\end{bmatrix}$$

$$(a_N^2+b_N^2+c_N^2+d_N^2=1) . \tag{12}$$

All the parameters in Eqs. (11) and (12) are real. We will assume that the consecutive pulses *do not overlap,* which requires that the repetition time T is sufficiently large to allow the individual pulses wings to vanish before the next pulse comes. Then since the probability amplitudes after the interaction of the atom with the kth pulse serve as initial conditions for the $(k+1)$st pulse, the $\mathbf{S}_N$ matrix is given by

$$\mathbf{S}_N=[\mathbf{S}_1]^N . \tag{13}$$

To find the $\mathbf{S}_1$ matrix, we consider the two-state equations

(7) in the time interval $[-T/2,T/2]$ in which the atom interacts with the first pulse only. They have the form

$$i\frac{dC_1(t)}{dt}=\tfrac{1}{2}\Omega(t)e^{-i\Lambda_0(t)}C_2(t)\ ,$$
$$i\frac{dC_2(t)}{dt}=\tfrac{1}{2}\Omega(t)e^{+i\Lambda_0(t)}C_1(t) \tag{14}$$

$(-\frac{1}{2}T\le t\le\frac{1}{2}T)$. Since the pulse wings are assumed to vanish outside $[-T/2,T/2]$, we can *formally* extend this interval to $(-\infty,\infty)$ and utilize the available single-pulse analytical solutions which are normally given in the form (10) for the sake of mathematical convenience. This is justified because in the interaction representation (2) the probability amplitudes $C_1(t)$ and $C_2(t)$ do not change in the absence of external fields, neither in modulus nor in phase. Given the single-pulse solution, one can construct the single-pulse interaction matrix

$$\mathbf{S}_{\rm int}=\begin{bmatrix} a+ib & c+id \\ -c+id & a-ib \end{bmatrix}\quad (a^2+b^2+c^2+d^2=1)\ . \tag{15}$$

It should be stressed that this is *not* the $\mathbf{S}_1$ matrix (11) involved in Eq. (13). The latter is a product of $\mathbf{S}_{\rm int}$ and a matrix $\mathbf{S}_{\rm free}$, which describes the phase shifts accumulated by the probability amplitudes during the repetition time T due to the free evolution of the system. To find $\mathbf{S}_{\rm free}$, let us consider the time interval $[T/2,3T/2]$ in which the atom interacts with the second pulse only. The two-state equations (7) in this time interval are

$$i\frac{dC_1(t)}{dt}=\tfrac{1}{2}\Omega(t-T)e^{-i\Lambda_1(t)}C_2(t)\ ,$$
$$i\frac{dC_2(t)}{dt}=\tfrac{1}{2}\Omega(t-T)e^{+i\Lambda_1(t)}C_1(t) \tag{16}$$

$(\frac{1}{2}T\le t\le\frac{3}{2}T)$. Since $\Lambda_1(t)=\Lambda_0(t-T)+\Lambda_1(T)$ [see Eq. (8)], by making a translation $t=t'+T$ and a substitution

$$C'_{1,2}(t')=C_{1,2}(t'+T)e^{\pm\frac{1}{2}i\Lambda_1(T)}\ ,$$

we find that Eqs. (16) are transformed into the same form as Eqs. (14) [which is required in order for Eq. (13) to be valid] but with amplitudes shifted in phase by $\frac{1}{2}\Lambda_1(T)$ for $C_1(t)$ and $-\frac{1}{2}\Lambda_1(T)$ for $C_2(t)$. This shift can be described by multiplication of $\mathbf{C}(t)$ with the free-evolution matrix

$$\mathbf{S}_{\rm free}=\begin{bmatrix} e^{i\varphi(T)} & 0 \\ 0 & e^{-i\varphi(T)} \end{bmatrix}\ , \tag{17}$$

where the phase shift is given by

$$\varphi(T)=\tfrac{1}{2}\Lambda_1(T)\quad\text{for pulse train (4a)}\ . \tag{18a}$$

When $\omega(t)=$const, i.e. for nonchirped pulses, the phase shift φ is equal to $\frac{1}{2}\Delta T$. For an interaction corresponding to field (4b), a similar analysis shows that the phase shift is

$$\varphi(T)=\tfrac{1}{2}\omega_a T\quad\text{for pulse train (4b)} \tag{18b}$$

for both chirped and nonchirped pulses. Therefore, the $\mathbf{S}_1$ matrix is given by

$$\mathbf{S}_1=\mathbf{S}_{\rm free}\mathbf{S}_{\rm int}\ . \tag{19}$$

From Eqs. (11), (15), (17), and (19) we obtain

$$a_1=a\cos\varphi-b\sin\varphi\quad b_1=a\sin\varphi+b\cos\varphi\ ,$$
$$c_1=c\cos\varphi-d\sin\varphi\quad d_1=c\sin\varphi+d\cos\varphi\ , \tag{20}$$

where

$$P_1^{(1)}=a_1^2+b_1^2=a^2+b^2\ ,$$
$$P_2^{(1)}=c_1^2+d_1^2=c^2+d^2=1-P_1^{(1)}$$

are the single-pulse–induced populations of levels $|1\rangle$ and $|2\rangle$, provided the initial conditions are given by Eqs. (9). $P_2^{(1)}$ represents the transition probability as well.

Since there are a number of analytical solutions to the two-state problem it is very useful to express the matrix elements of $\mathbf{S}_N$ in terms of those of $\mathbf{S}_1$. This would allow analytical treatment of the excitation by N identical pulses given the single-pulse solutions. Using Eq. (13) and the unitarity of $\mathbf{S}_1$ and $\mathbf{S}_N$, in the Appendix we have derived the relations between the elements of $\mathbf{S}_N$ and $\mathbf{S}_1$ which have the form (A1)

$$a_N=\cos N\vartheta,\quad b_N=b_1\frac{\sin N\vartheta}{\sin\vartheta}\ ,$$
$$c_N=c_1\frac{\sin N\vartheta}{\sin\vartheta},\quad d_N=d_1\frac{\sin N\vartheta}{\sin\vartheta}\ , \tag{21}$$

where

$$\vartheta=\arccos a_1\quad(0\le\vartheta<\pi)\ . \tag{22}$$

It can be shown that the quantities $\cos N\vartheta$ and $\sin(N\vartheta)/\sin\vartheta$ are polynomials of a_1 given by [32]

$$\frac{\sin N\vartheta}{\sin\vartheta}=\begin{cases}\displaystyle\sum_{k=0}^{n-1}(-)^{n+k-1}\frac{(n+k)!}{(n-k-1)!(2k+1)!}(2a_1)^{2k+1} & (N=2n)\ ,\\ \displaystyle\sum_{k=0}^{n}(-)^{n+k}\frac{(n+k)!}{(n-k)!(2k)!}(2a_1)^{2k} & (N=2n+1)\ ,\end{cases}$$

$$\cos N\vartheta=\begin{cases}\displaystyle n\sum_{k=0}^{n}(-)^{n+k}\frac{(n+k-1)!}{(n-k)!(2k)!}(2a_1)^{2k} & (N=2n)\ ,\\ \displaystyle(n+\tfrac{1}{2})\sum_{k=0}^{n}(-)^{n+k}\frac{(n+k)!}{(n-k)!(2k+1)!}(2a_1)^{2k+1} & (N=2n+1)\ .\end{cases}$$

Inasmuch as the parameters (21) of the S_N matrix depend on the phase shift φ through $\sin\varphi$ and $\cos\varphi$ only [Eqs. (22) and (20)], for simplicity and without loss of generality we will assume that $0 \le \varphi \le 2\pi$ in what follows unless otherwise specified.

E. General properties of the transition probability

Provided the system is prepared initially in state $|1\rangle$, the populations of the two states induced by the pulse train are given by

$$P_1^{(N)} = a_N^2 + b_N^2 = 1 - P_2^{(1)} \frac{\sin^2 N\vartheta}{\sin^2\vartheta} , \tag{23a}$$

$$P_2^{(N)} = c_N^2 + d_N^2 = P_2^{(1)} \frac{\sin^2 N\vartheta}{\sin^2\vartheta} . \tag{23b}$$

The population $P_2^{(N)}$ of the upper state $|2\rangle$ equals the transition probability. Relation (23b) shows that $P_2^{(N)}$ is equal to the single-pulse transition probability $P_2^{(1)}$ times a factor that represents the interference effect of the pulse train. It is worth discussing some general properties and limiting cases of $P_2^{(N)}$.

We should point out that in the case of a single pulse, the free evolution of the system before and after the interaction with the pulse does not influence the populations. For more than one pulse, however, although the free evolution before and after the pulse train is of no importance, the free evolution *during and between* the pulses explicitly affects the populations via the repetition time T. In fact, this is the physical basis of the theory of Ramsey fringes [5]. It should be pointed out that it is the phase shift φ that makes the transition probabilities for fields (4a) and (4b) different. In the case of (4a), φ depends on the laser frequency ω through the detuning $\Delta = \omega_a - \omega$ via Eqs. (18a) and (8). In the case of field (4b), the phase shift $\varphi = \frac{1}{2}\omega_a T$ does not depend on ω. Therefore, the populations regarded as functions of Δ (and thence, of ω) are expected to show much more complicated features for field (4a) than for field (4b). On the other hand, regarded as functions of the pulse area A, the populations induced by trains (4a) and (4b) do not differ in principle because φ does not depend on A; the same phase shift can be obtained by appropriate choice of the repetition time T [generally different for fields (4a) and (4b)].

When the excitation is weak (small pulse area), that is when $a \approx 1$, $|b|, |c|, |d| \ll 1$, from Eqs. (20) we obtain $a_1 \approx a\cos\varphi \approx \cos\varphi$. Then Eq. (22) suggests that $\vartheta \approx \varphi$ and the train-induced transition probability is

$$P_2^{(N)} \approx P_2^{(1)} \frac{\sin^2 N\varphi}{\sin^2\varphi} . \tag{24a}$$

For the particular case of Gaussian pulses with the electric field (4b) when $\varphi = \frac{1}{2}\omega_a T$, this result is reduced to formula (4c) of Thomas [13] (apart from a factor of $\frac{1}{2}$ misprinted in Ref. [13]). We should stress that the train-induced factor (the fraction) in the approximate formula (24a) depend on the free-evolution phase shift φ only while in the exact formula (23b) it also depends on the interaction dynamics, i.e. on a_1 (20), through ϑ (22). Simple results are obtained when the $\varphi = m\pi$ (where m is an integer). Then

$$P_2^{(N)} \approx P_2^{(1)} N^2 , \tag{24b}$$

i.e., *in the limit of weak excitation and for a free-evolution phase shift equal to an integer multiple of π, the transition probability is proportional to the squared number of pulses N^2*, in agreement with earlier conclusions based on perturbation theory [9–11,13].

It is worth noting that formula (24a) contains Salour's results [9,10] for weak excitation with two pulses. Really, for $N = 2$, Eq. (24a) gives

$$P_2^{(2)} = 4P_2^{(1)}\cos^2\varphi$$

and with phases (18a) and (18b), corresponding to pulse trains (4a) and (4b), we obtain Salour's formulas (13) and (25) in Ref. [10], respectively.

Another interesting observation is that Eq. (23b) resembles very much the intensity distribution for a diffraction grating. That is, *the interaction of a two-state system with a train of pulses is a quantum analog of the diffraction grating in optics.* Qualitatively, such a conjecture has been made earlier [8–10] in the case of weak excitation. Eq. (23b) is the rigorous form of this property. It is a general result for *any* pulse shape, pulse area, and detuning. It should be pointed out that the analogy is not absolute because, in contrast to the case of a diffraction grating, $P_2^{(1)}$ in Eq. (23b) depends on the same parameters as ϑ, i.e., on the detuning, the pulse area, and the pulse shape. The most important difference is the absence of the large peaks at $\vartheta = m\pi$ (where m is an integer), characterizing the diffraction-grating pattern. Really, in the present case $\vartheta = m\pi$ means that $|a_1| = 1$ [see Eq. (22)], which implies $P_1^{(1)} = 1$ and $P_2^{(1)} = 0$ and hence, $P_2^{(N)} = 0$, i.e., at $\vartheta = m\pi$ the transition probability $P_2^{(N)}$ equals zero but not a maximum.

Finally, it should be pointed out that small changes in the interaction parameters, and consequently, in S_1 (11) and in turn in ϑ (22) via a_1, are enhanced N times in the train-induced populations (23). In other words, $P_2^{(N)}$ is much more sensitive to such changes than the single-pulse probability $P_2^{(1)}$.

F. Conditions for complete population inversion and return

It is particularly interesting to consider the cases of complete population inversion (CPI), when $P_1^{(N)} = 0$ and $P_2^{(N)} = 1$, and complete population return (CPR), when $P_1^{(N)} = 1$ and $P_2^{(N)} = 0$.

Complete population inversion requires $a_N = 0$ and $b_N = 0$. Since $\sin(N\vartheta)/\sin\vartheta$ should not be zero [else $c_N = d_N = 0$, which contradicts $P_2^{(N)} = c_N^2 + d_N^2 = 1$; see Eqs. (21) and (23)], the second of these conditions is equivalent to $b_1 = 0$. Hence CPI occurs when both conditions

$$a_1 = \cos\frac{(2k-1)\pi}{2N} \quad (k = 1, 2, \ldots, N) , \tag{25a}$$

$$b_1 = 0 \tag{25b}$$

are satisfied. They are to be considered as a system of two equations for the pulse-train parameters: detuning, pulse area, pulse shape, and repetition time.

Complete population return requires $c_N=0$ and $d_N=0$. These conditions are satisfied when

$$c_1=0 \quad \text{and} \quad d_1=0 \tag{26}$$

or when

$$a_1=\cos\frac{k\pi}{N} \quad (k=1,2,\ldots,N-1) . \tag{27}$$

The former is the condition for CPR in the case of a single pulse [see Eq. (11)]. This is the trivial solution that suggests that if CPR occurs for a single pulse it will occur for N pulses as well. The latter condition, which results from quantum interference, generates additional nodes in $P_2^{(N)}$.

In Secs. III–VI we apply the general results obtained above to four specific important cases: resonant, rectangular, Rosen-Zener, and Allen-Eberly pulses, respectively.

III. EXACT RESONANCE

In the case of exact resonance the detuning is zero, $\Delta\equiv 0$, and the parameters of the single-pulse matrix $\mathbf{S}_1$ (11) are given by

$$a_1=\cos\tfrac{1}{2}A\cos\varphi, \quad b_1=\cos\tfrac{1}{2}A\sin\varphi ,$$

$$c_1=\sin\tfrac{1}{2}A\sin\varphi, \quad d_1=-\sin\tfrac{1}{2}A\cos\varphi ,$$

where A is the pulse area

$$A=\int_{-\infty}^{\infty}\Omega(t)dt$$

and $\Omega(t)$ has an arbitrary shape with rapidly vanishing wings. The single-pulse transition probability is

$$P_2^{(1)}=\sin^2\tfrac{1}{2}A . \tag{28}$$

The elements of the $\mathbf{S}_N$ matrix (12) are given by Eqs. (21) with ϑ being

$$\vartheta=\arccos(\cos\tfrac{1}{2}A\cos\varphi) \quad (0\le\vartheta<\pi) . \tag{29}$$

For field (4a), $\varphi=\frac{1}{2}\Delta T=0$; then

$$P_1^{(N)}=\cos^2\tfrac{1}{2}NA, \quad P_2^{(N)}=\sin^2\tfrac{1}{2}NA . \tag{30}$$

Equations (30) hold for field (4b) only provided $\varphi=\frac{1}{2}\omega_a T=m\pi$ (where m is an integer); this can be explained in terms of constructive interference. Equations (30) show that the number of oscillations in the populations induced by N pulses is N times larger than the number of oscillations for a single pulse, the transition probability being a sinusoid with a period of $2\pi/N$. The populations oscillate between zero and one and CPI occurs at $A=(2k-1)\pi/N$ $(k=1,2,\ldots)$ while CPR at $A=2k\pi/N$ $(k=1,2,\ldots)$. These results can be easily generalized for resonant pulses of nonequal areas.

However, one should keep in mind that for the field (4b) this simple picture is only valid if $\frac{1}{2}\omega_a T=m\pi$.

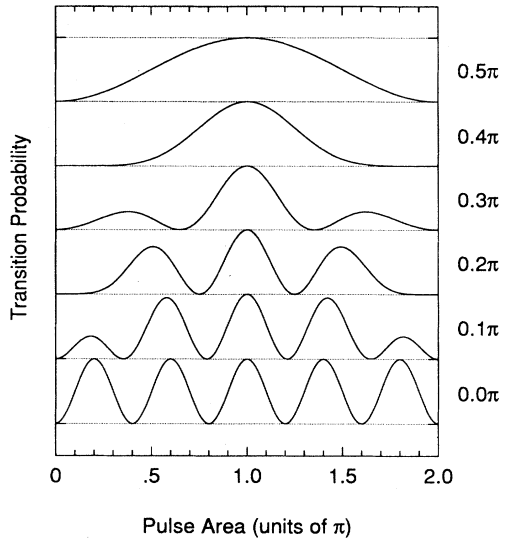

FIG. 1. The transition probability against the single-pulse area A in the case of a train of $N=5$ resonant pulses with an electric field given by Eq. (4b) for several different values (denoted by numbers on the right of the figure) of the free-evolution phase shift φ between 0 and $\frac{1}{2}\pi$. The probability is a periodic function of the pulse area with a period of 2π. For each curve, the adjacent horizontal dotted lines indicate the values of zero and unity probability.

When this condition is not fulfilled the populations are given by Eqs. (23) with ϑ (29). In Figs. 1 and 2 the transition probability is plotted against the pulse area for a number of values of the phase $\varphi=\frac{1}{2}\omega_a T$ between 0 and $\frac{1}{2}\pi$ in the cases of 5 and 6 pulses. In the interval $[\frac{1}{2}\pi,\pi]$ the situation is similar, as $P_2^{(N)}$ is invariant under the change of φ by $\pi-\varphi$. The region $0\le A\le 2\pi$ is only shown because the transition probability is a periodic

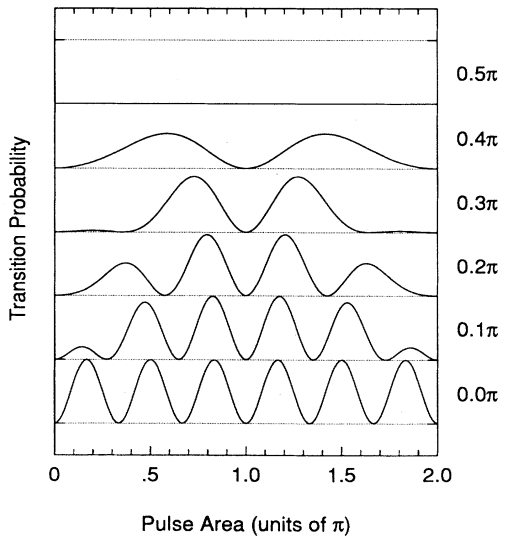

FIG. 2. The same as Fig. 1 but for $N=6$ pulses.

function of A with a period of 2π. When $\varphi=0$ we obtain pure sinusoids with periods of $2\pi/5$ and $2\pi/6$ as discussed above. At $\varphi=\pi/2$ we have $\vartheta=\pi/2$ and hence, $P_2^{(N)}=\sin^2(\frac{1}{2}A)\sin^2(\frac{1}{2}N\pi)$. Thus, for N even and $\varphi=\pi/2$, the transition probability is identically equal to zero as seen in Fig. 2, which can be explained as a result of destructive interference. For N odd and $\varphi=\pi/2$, it equals the single-pulse one (28) as shown in Fig. 1. Between φ equal to 0 and $\pi/2$, $P_2^{(N)}$ passes from one limiting case to another.

IV. RECTANGULAR PULSES

In the case of a single symmetric pulse of constant nonzero detuning the transitions are of nonadiabatic nature and the excited-state population $P_2^{(1)}$ generally decreases when increasing the detuning. As a function of the pulse area A, $P_2^{(1)}$ oscillates between zero and certain values below unity, CPR being a typical feature while CPI appears to be impossible, at least in the models studied so far. It turns out that this limitation is removed when a two-state system interacts with more than one such pulse. In this section, we consider rectangular pulses and in the next, Rosen-Zener pulses. It is interesting to compare the excitation spectra induced by trains of such pulses because the Rosen-Zener pulses are smooth and hence, much more adiabatic. We will see that the two kinds of pulses lead to quite different results at large detuning.

A. The transition probability

The Rabi frequency and the detuning of a train of N rectangular pulses are given by

$$\Omega(t)=\begin{cases}\dfrac{A}{\tau} & \text{for } kT-\frac{1}{2}\tau\le t\le kT+\frac{1}{2}\tau \quad (k=0,1,\ldots,N-1)\ ,\\ 0 & \text{anywhere else}\ ,\end{cases} \tag{31a}$$

$$\Delta(t)=\delta/\tau\ , \tag{31b}$$

where τ is the pulse width, which also plays the role of a time-scale parameter, T is the repetition time ($T>\tau$), A is the single pulse area, and δ is a dimensionless constant detuning. The elements (20) of the $\mathbf{S}_1$ matrix (11) are

$$\begin{aligned} a_1&=\sqrt{1-P_2^{(1)}}\cos\xi,\quad c_1=\frac{A}{\sqrt{A^2+\delta^2}}\sin\tfrac{1}{2}\sqrt{A^2+\delta^2}\sin\varphi\ ,\\ b_1&=\sqrt{1-P_2^{(1)}}\sin\xi,\quad d_1=-\frac{A}{\sqrt{A^2+\delta^2}}\sin\tfrac{1}{2}\sqrt{A^2+\delta^2}\cos\varphi\ , \end{aligned} \tag{32}$$

where

$$\xi=-\tfrac{1}{2}\delta+\arctan\left[\frac{\delta}{\sqrt{A^2+\delta^2}}\tan\tfrac{1}{2}\sqrt{A^2+\delta^2}\right]+\varphi\ . \tag{33}$$

The free-evolution phase φ equals $\delta T/2\tau$ for train (4a) and $\frac{1}{2}\omega_a T$ for train (4b). The single-pulse transition probability is given by [33]

$$P_2^{(1)}=\frac{A^2}{A^2+\delta^2}\sin^2\tfrac{1}{2}\sqrt{A^2+\delta^2}\ . \tag{34}$$

The parameters of the $\mathbf{S}_N$ matrix (12) can be obtained from Eqs. (21) with ϑ (22) and a_1 (32). The populations $P_1^{(N)}$ and $P_2^{(N)}$ induced by a train of N rectangular pulses are given by Eqs. (23).

B. Complete population inversion

As a function of the pulse area, the single-pulse transition probability (34) oscillates with an amplitude that increases with A. As a function of the detuning δ, it oscillates with a Lorentzian modulation of the amplitude. $P_2^{(1)}$ is always less than unity provided $\delta\neq0$, although it can be very close to 1 when $A\gg\delta$. For two and more pulses CPI becomes possible. According to Eqs. (25) and (32) it occurs whenever

$$\sqrt{1-P_2^{(1)}}\cos\xi=\cos\frac{(2k-1)\pi}{2N}\quad (k=1,2,\ldots,N) \tag{35a}$$

$$\sin\xi=0\ . \tag{35b}$$

Substituting Eq. (35b) into Eq. (35a) gives

$$\frac{A}{\sqrt{A^2+\delta^2}}\left|\sin\tfrac{1}{2}\sqrt{A^2+\delta^2}\right|=\sin\frac{(2k-1)\pi}{2N}\quad (k=1,2,\ldots,N)\ .$$

It is easy to see that for any detuning and for any number of pulses $N>1$, this condition is satisfied by an infinite number of values of the pulse area. On the other hand, since the sin factor on the left-hand side (LHS) is always ≤1, one can show that this equation imposes an upper limit on $|\delta|/A$ for CPI

$$\frac{|\delta|}{A} \leq \cot\frac{\pi}{4N} . \tag{36}$$

At large N the right-hand side (RHS) increases approximately linearly with N. This means that for a given detuning δ, CPI is possible for a sufficiently large pulse area A or for large enough N.

C. Dependence on the detuning

For field (4a) the transition probability is an even function of the detuning δ because $\varphi=\delta T/2\tau$ [see Eqs. (32)–(34)]. In Figs. 3 and 4 the transition probability for train (4a) is plotted against the detuning for pulse areas of π and 2π, respectively, and a train repetition time of $T=10\tau$. The difference between the two figures is most noticeable near resonance, $\delta=0$. As is well known, at $\delta=0$ the single-pulse transition probability has a maximum equal to unity for $A=\pi$, while for $A=2\pi$ it is zero. Consequently, for $A=2\pi$, $P_2^{(N)}$ is equal to zero at resonance [see the discussion of Eq. (26)]. For $A=\pi$, $P_2^{(N)}$ equals unity for odd N and zero for even N; this is because any consecutive π pulse swaps the atomic populations. Off resonance, the two figures do not differ substantially. For $N\geq 2$, the transition probability oscillates rapidly due to the $\sin^2(N\vartheta)/\sin^2\vartheta$ factor in Eq. (23b) and because ϑ depends on δ through ξ [see Eqs. (22), (32), and (33)]. These oscillations are modulated in amplitude by the single-pulse transition probability $P_2^{(1)}$, which is clearly seen in the figures. Furthermore, we should note the overall increase of the amplitude of the oscillations, the rise in their complexity, and the narrowing of the structures when the number of pulses increases. Finally, the situation is generally similar to Figs. 3 and 4 when A is equal to an odd or even multiple of π, respectively. When A is between these values the picture is not substantially different far from resonance while near $\delta=0$ it is somewhere between Figs. 3 and 4.

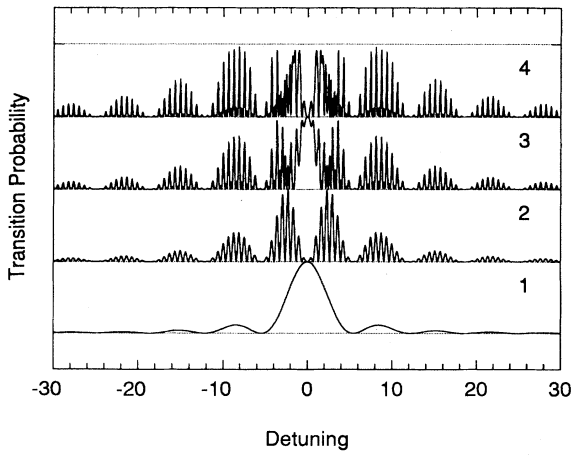

FIG. 3. The transition probability against the dimensionless detuning δ for a train of one to four rectangular pulses (31) each of area $A=\pi$. The numbers of the pulses are indicated in the figure. The electric field is given by Eq. (4a) and the train repetition rate is $T=10\tau$ where τ is the pulse width.

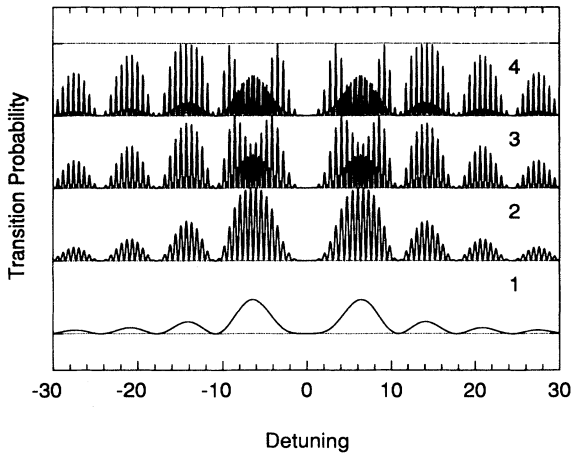

FIG. 4. The same as Fig. 3 but for a single-pulse area of 2π.

D. Dependence on the free-evolution phase shift

The situation differs markedly for the pulse train (4b) when $\varphi=\frac{1}{2}\omega_a T$. First, plotted against the detuning δ, the transition probability $P_2^{(N)}$ is generally an asymmetric function due to the explicit dependence of ξ (33) [and in turn, of a_1 (32) and $P_2^{(N)}$ (23b)] on φ. Second, $P_2^{(N)}$ exhibits much fewer oscillations compared to the case of train (4a) considered above because φ does not depend on δ. For field (4a), it is the term $\varphi=\delta T/2\tau$ in ξ which changes most rapidly with δ, thus generating lots of oscillations in $P_2^{(N)}$. In the same time, $P_2^{(N)}$ strongly depends on φ. It is plotted in Fig. 5 for various values of φ from 0 to π for $N=5$ pulses each of area of π. The figure shows that the

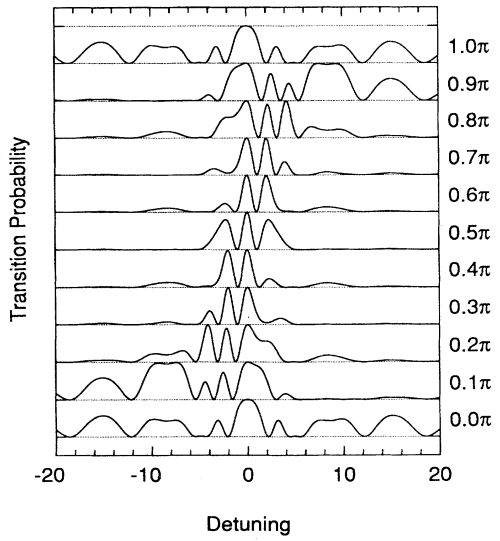

FIG. 5. The transition probability against the dimensionless detuning δ for a train of five rectangular pulses (31) each of area of π for several different values of the free-evolution phase shift φ between 0 and π (the numbers on the right of the figure). For each curve, the adjacent horizontal dotted lines indicate the values of zero and unity probability. The electric field is given by Eq. (4b).

transition probability is symmetric for φ equal to 0, $\pi/2$, and π. In the case of $\varphi=0$ the explanation is trivial. For $\varphi=\pi$, the symmetry is kept simply because $\varphi=\pi$ gives the same $P_2^{(N)}$ as $\varphi=0$, which is easily proved. For $\varphi=\pi/2$, the change $\delta\rightarrow-\delta$ leads to changes $\xi\rightarrow\pi-\xi$, $a_1\rightarrow-a_1$, $\vartheta\rightarrow\pi-\vartheta$ and $P_2^{(N)}$ (23b) does not change.

V. ROSEN-ZENER PULSES

A. The transition probability

In the model of Rosen and Zener [29] the Rabi frequency and the detuning of a single pulse are given by

$$\Omega(t)=\frac{A}{\pi\tau}\operatorname{sech}\frac{t}{\tau},\quad \Delta(t)=\frac{\delta}{\tau}\ , \tag{37}$$

where $\tau>0$ is a time-scale parameter, $A>0$ is the single-pulse area, and δ is a dimensionless scaled constant detuning. Our choice of this model is due to the fact that first, it offers a realistic and smooth pulse shape and second, it provides a simple analytical solution. The parameters (20) of the $\mathbf{S}_1$ matrix (11) are given by

$$\begin{aligned} a_1&=\sqrt{1-P_2^{(1)}}\cos\xi,\quad c_1=\operatorname{sech}\tfrac{1}{2}\pi\delta\sin\tfrac{1}{2}A\sin\varphi\ ,\\ b_1&=\sqrt{1-P_2^{(1)}}\sin\xi,\quad d_1=-\operatorname{sech}\tfrac{1}{2}\pi\delta\sin\tfrac{1}{2}A\cos\varphi\ , \end{aligned} \tag{38}$$

with

$$\xi=\arg\frac{\Gamma^2[\frac{1}{2}+\frac{1}{2}i\delta]}{\Gamma[\frac{1}{2}+\frac{1}{2}\alpha+\frac{1}{2}i\delta]\Gamma[\frac{1}{2}-\frac{1}{2}\alpha+\frac{1}{2}i\delta]}+\varphi\ , \tag{39}$$

where $\alpha=A/\pi$ and $\Gamma(z)$ is the gamma function. The free-evolution phase shift φ equals $\delta T/2\tau$ for train (4a) and $\frac{1}{2}\omega_a T$ for train (4b). The single-pulse transition probability is [29]

$$P_2^{(1)}=\operatorname{sech}^2\tfrac{1}{2}\pi\delta\sin^2\tfrac{1}{2}A\ . \tag{40}$$

The parameters of the $\mathbf{S}_N$ matrix (12) can be obtained from Eqs. (21) with ϑ (22) and a_1 (38). The populations $P_1^{(N)}$ and $P_2^{(N)}$ induced by a train of N Rosen-Zener pulses are given by Eqs. (23).

An important difference between Eq. (40) and transition probability (34) for a single rectangular pulse is that the former decreases much faster against the detuning, namely, exponentially, compared with the Lorentzian decrease of the latter. This is because the Rosen-Zener pulses (37) are smooth and hence, much more adiabatic than the rectangular ones (31). We will see that this leads to quite different results in the case of pulse trains as well. Furthermore, an interesting peculiarity of the Rosen-Zener probability (40) is the factorization of the dependences on the pulse area A and the detuning δ. This fact greatly simplifies analysis of the effects induced by Rosen-Zener pulses.

B. Dependence on the detuning

As for the rectangular pulses, the transition probability is an even function of the detuning δ for train (4a) because $\varphi=\delta T/2\tau$. For train (4b), however, $P_2^{(N)}$ is asymmetric in general.

In Fig. 6, the transition probability is plotted against the detuning for a pulse area of π, at which the single-pulse transition probability (40) is maximum, and a train repetition rate of $T=10\tau$. As Eq. (40) suggests the single-pulse transition probability is a bell-shaped function of the detuning without any oscillations, in contrast to the case of a rectangular pulse. At resonance, $P_2^{(N)}$ equals unity for odd N and zero for even N because any consecutive π pulse swaps the atomic populations. The number of oscillations increases with the number of pulses while their width decreases. Outside the shown detuning range $P_2^{(N)}$ is very small. The picture is generally much simpler than for the rectangular pulses (Fig. 3). This is due to first, the absence of a dependence on the detuning in the oscillating sine factor in Eq. (40), and second, the rapidly vanishing wings of $P_2^{(1)}$, which modulates $P_2^{(N)}$ through Eq. (23b). The latter property does not allow large-detuning oscillations such as the ones in Figs. 3 and 4. We should mention that the situation is similar to Fig. 6 when the pulse area A equals an odd multiple of π. When A equals an even multiple of π, according to Eqs. (23b) and (40) the transition probability is identically equal to zero for any detuning and any number of pulses. This is a substantial difference compared to the rectangular pulses (Fig. 4). Between these values, the situation is similar to Fig. 6, the oscillations being generally smaller in amplitude.

As for the rectangular pulses, the situation is markedly different for train (4b) when $\varphi=\frac{1}{2}\omega_a T$. First of all, plotted against δ, $P_2^{(N)}$ exhibits fewer oscillations compared to train (4a) because φ does not change when varying the

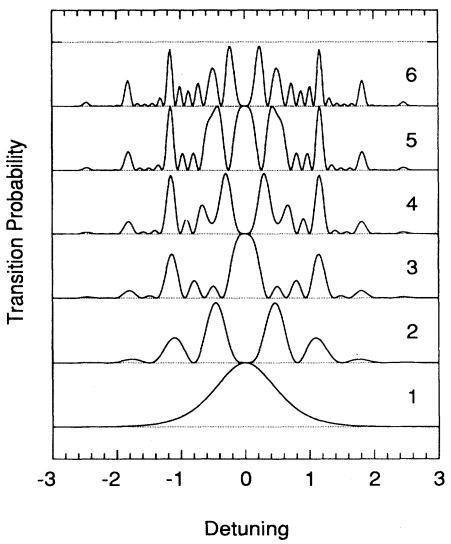

FIG. 6. The transition probability against the dimensionless detuning δ for a train of one to six Rosen-Zener pulses (37) (indicated by the numbers on the right of the figure) each of area of π. The electric field is given by Eq. (4a) and the train repetition time is $T=10\tau$. Note the difference in the detuning scale compared to the corresponding Fig. 3 for rectangular pulses. For each curve, the adjacent horizontal dotted lines indicate the values of zero and unity probability.

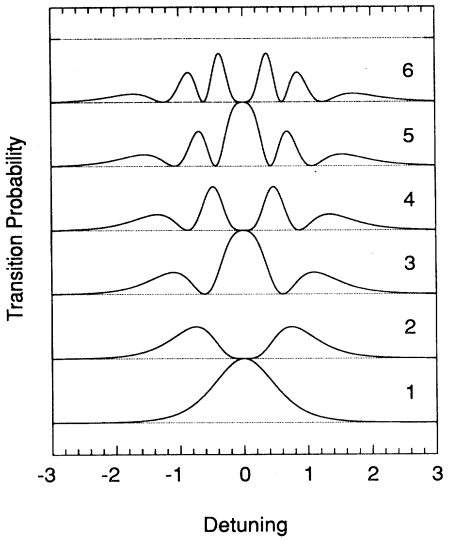

FIG. 7. The same as Fig. 6 but for field (4b) with $\varphi=0$.

detuning δ. Such a case is shown in Fig. 7 where $P_2^{(N)}$ is plotted against the detuning, which is assumed to vary through the laser frequency ω, for $\varphi=0$. Figure 7 is markedly simpler than Fig. 6 corresponding to train (4a). For field (4a), it is the term $\varphi=\delta T/2\tau$ in ξ (39) that changes most rapidly with δ, thus generating lots of small oscillations in $P_2^{(N)}$. On the other hand, for arbitrary φ, $P_2^{(N)}$ is an asymmetric function due to the presence of the (constant) phase $\varphi=\frac{1}{2}\omega_a T$ in ξ (39) (φ does not change with δ and hence, breaks the symmetry). In Fig. 8, the transition probability is plotted for $N=5$ pulses, each of

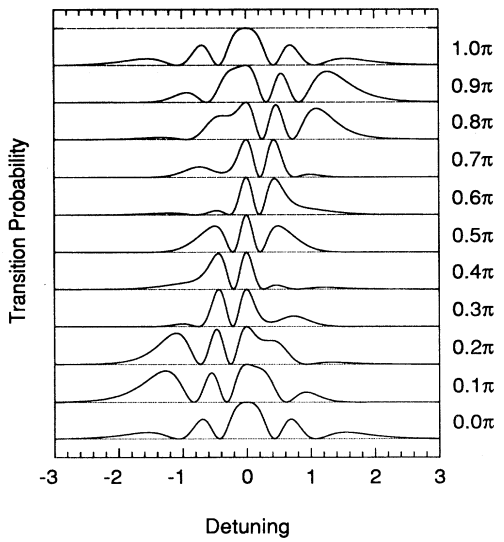

FIG. 8. The transition probability against the dimensionless detuning δ for a train of five Rosen-Zener pulses (37) each of area of π for several different values of the free-evolution phase shift φ between 0 and π (the numbers on the right of the figure). For each curve, the adjacent horizontal dotted lines indicate the values of zero and unity probability. The electric field is given by Eq. (4b).

area of π, for various values of φ from 0 to π. Values of φ from 0 to π are only shown because $P_2^{(N)}$ is a periodic function of φ with a period of π. The figure shows that the transition probability is symmetric for φ equal to 0, $\pi/2$, and π. The explanation is similar to that for rectangular pulses.

C. Dependence on the pulse area

As a function of the pulse area A, the single-pulse transition probability (40) oscillates between 0 and its constant maximum value $\mathrm{sech}^2(\frac{1}{2}\pi\delta)<1$ ($\delta\neq 0$), which shows that complete population inversion is not possible unless $\delta=0$ (exact resonance). In the case of two and more pulses, however, CPI becomes possible. Because of $P_2^{(1)}<1$ for $\delta\neq 0$ [see Eq. (40)], the second CPI condition (25b) is satisfied when [see Eqs. (38)]

$$\sin\xi(A,\delta)=0\ . \tag{41a}$$

Then the first CPI condition (25a) transforms into

$$|\sin\tfrac{1}{2}A|=\cosh\tfrac{1}{2}\pi\delta\,\sin\frac{(2k-1)\pi}{2N}\quad(k=1,2,\ldots,N)\ . \tag{41b}$$

CPI conditions (41a) and (41b) are to be considered as a system of equations for A and δ. This system is easily reduced to one equation by solving Eq. (41b) for δ and substituting the value into Eq. (41a). A number of pairs (A,δ) for which CPI occurs are presented in Table I. In Fig. 9, the transition probability for train (4b) with $\varphi=0$ is plotted as a function of the pulse area A for $\delta\approx 0.9774$. For this choice, CPI occurs for $N=4$ at $A\approx 3.2403\pi$ (see

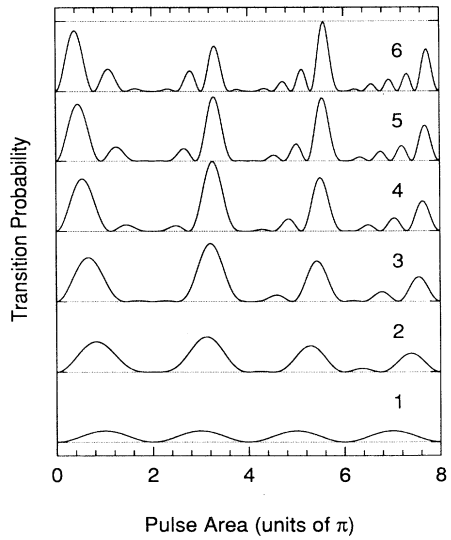

FIG. 9. The transition probability against the pulse area A for a train of one to six Rosen-Zener pulses (37) (indicated on the right of the figure) for a detuning of $\delta\approx 0.9774$. The electric field is given by Eq. (4b) and the free-evolution phase shift φ is equal to zero. For this detuning, complete population inversion is realized for $N=4$ pulses at $A\approx 3.2403\pi$. For each curve, the adjacent horizontal dotted lines indicate the values of zero and unity probability.

TABLE I. Some approximate CPI solutions for 2, 3, 4, and 5 Rosen-Zener pulses (37) for pulse train (4b) with $\varphi=0$.

2 pulses		3 pulses		4 pulses		5 pulses	
A	δ	A	δ	A	δ	A	δ
2.7957π	0.5126	3.0829π	0.8321	3.2403π	0.9774	3.3430π	1.0700
4.9727π	0.5603	5.2539π	0.7774	5.4026π	0.8767	5.4972π	0.9385
7.0565π	0.5575	7.3295π	0.7324	7.4715π	0.8116	7.5606π	0.8602
9.1071π	0.5482	9.3735π	0.6988	9.5106π	0.7665	9.5960π	0.8076

Table I). It is seen from the figure that the number of oscillations in $P_2^{(N)}$ increases with the number of pulses. Furthermore, the amplitude of these oscillations increases too, which in fact makes CPI possible. One also finds that the oscillations are clearly modulated in amplitude by the single-pulse probability $P_2^{(1)}$, as expected from Eq. (23b).

An important conclusion from the CPI condition (41b) is that it imposes *an upper limit on the detuning*. Since $|\sin\frac{1}{2}A|\leq 1$, after simple calculations one can show that Eq. (41b) leads to the following restriction on $|\delta|$:

$$|\delta|\leq\frac{2}{\pi}\ln\left[\cot\frac{\pi}{4N}\right]. \tag{42}$$

This upper limit increases nearly logarithmically with the number of pulses.

According to Eqs. (26) and (27) complete population return with N Rosen-Zener pulses occurs when

$$\operatorname{sech}\tfrac{1}{2}\pi\delta\sin\tfrac{1}{2}A=0$$

or when

$$\sqrt{1-\operatorname{sech}^2\tfrac{1}{2}\pi\delta\sin^2\tfrac{1}{2}A}\ \cos\xi(A,\delta)=\cos\frac{k\pi}{N}$$
$$(k=1,2,\ldots,N-1).$$

The former is just the condition for single-pulse CPR: $A=2m\pi$ $(m=1,2,\ldots)$. The latter condition results from quantum interference. A number of cases of CPR can be seen in Figs. 6–9. Of course, these cases are not as interesting as those of CPI because CPR is a typical property of the single Rosen-Zener pulses while CPI is impossible.

VI. CHIRPED PULSES: ALLEN-EBERLY MODEL

In this section we consider chirped-pulse excitation when the transitions occur due to crossing of the diabatic energy curves (Landau-Zener transitions). We have to note that the Landau-Zener model itself [34] does not represent a case of pulsed excitation since $\Omega(t)=$const there. Typically, as a function of the pulse area A, the excited-state population increases monotonically until some value of A and then oscillates between one and a given nonzero value with an amplitude that rapidly decreases when increasing the detuning.

A. The transition probability

We will consider multiple-pulse excitation by Allen-Eberly pulses [1,30,31] in which the Rabi frequency and the detuning of a single pulse are given by

$$\Omega(t)=\frac{A}{\pi\tau}\operatorname{sech}\frac{t}{\tau},\quad \Delta(t)=\frac{B}{\pi\tau}\tanh\frac{t}{\tau}, \tag{43}$$

where τ is a positive parameter defining the time scale, $A>0$ is the single-pulse area, and the real dimensionless parameter B determines the detuning slope at $t=0$ as well as the detuning value at $t\rightarrow\pm\infty$. Our choice of the Allen-Eberly model (43) is due to the fact that first, this model represents a realistic chirped pulse and second, it provides relatively simple expressions for the parameters (20) of the $\mathbf{S}_1$ matrix (11). These parameters are given by

$$\begin{aligned} a_1&=\operatorname{sech}\tfrac{1}{2}B\cos\tfrac{1}{2}\sqrt{A^2-B^2}\cos\varphi,\quad c_1=\sqrt{1-P_1^{(1)}}\sin\eta,\\ b_1&=\operatorname{sech}\tfrac{1}{2}B\cos\tfrac{1}{2}\sqrt{A^2-B^2}\sin\varphi,\quad d_1=-\sqrt{1-P_1^{(1)}}\cos\eta, \end{aligned} \tag{44}$$

where

$$\eta=\arg\frac{\Gamma^2[\frac{1}{2}+i\beta]}{\Gamma^2[\frac{1}{2}+\sqrt{\alpha^2-\beta^2}+i\beta]\Gamma^2[\frac{1}{2}-\sqrt{\alpha^2-\beta^2}+i\beta]}+\beta\ln 2+\varphi \tag{45}$$

with $\alpha=A/2\pi$ and $\beta=B/2\pi$. According to Eqs. (18), the phase shift φ equals $-\beta\ln[\cosh(T/\tau)]$ for train (4a) and $\frac{1}{2}\omega_a T$ for train (4b). The square roots in a_1, b_1, and η are real provided $A\geq|B|$ (we call this the *high-intensity region*) and imaginary if $A<|B|$ (we call this the *low-intensity region*). Since $\cos(ix)=\cosh x$, the single-pulse–induced populations are

$$P_1^{(1)}=\begin{cases}\operatorname{sech}^2\tfrac{1}{2}B\cosh^2\tfrac{1}{2}\sqrt{B^2-A^2} & (A<|B|),\\ \operatorname{sech}^2\tfrac{1}{2}B\cos^2\tfrac{1}{2}\sqrt{A^2-B^2} & (A\geq|B|),\end{cases} \tag{46a}$$

$$P_2^{(1)}=1-P_1^{(1)}=\begin{cases}1-\operatorname{sech}^2\frac{1}{2}B\cosh^2\frac{1}{2}\sqrt{B^2-A^2} & (A<|B|)\,,\\ 1-\operatorname{sech}^2\frac{1}{2}B\cos^2\frac{1}{2}\sqrt{A^2-B^2} & (A\geq|B|)\,.\end{cases} \tag{46b}$$

The parameters of the $\mathbf{S}_N$ matrix (12) can be obtained from Eqs. (21) with ϑ defined by Eq. (22) and a_1 given by Eq. (44). The populations $P_1^{(N)}$ and $P_2^{(N)}$ induced by a train of N pulses are then given by Eqs. (23). It is worth noting that the populations do not depend on the phase η (45), neither for a single pulse nor for a pulse train.

As a function of the pulse area A, the single-pulse transition probability (46b) increases monotonically in the low-intensity region ($A<|B|$) and then in the high-intensity region ($A\geq|B|$) oscillates between one and $[P_2^{(1)}]_{\min}=1-\operatorname{sech}^2(\frac{1}{2}B)>0$, regularly reaching complete population inversion. The oscillations amplitude, $\operatorname{sech}^2(\frac{1}{2}B)$, decreases exponentially when increasing the detuning slope B, the excitation becoming increasingly adiabatic. It is clear from Eqs. (46) that complete population return is not possible in the case of a single Allen-Eberly pulse unless $B=0$ (exact resonance) or $A=0$ (no pulse). However, for two and more pulses CPR becomes possible as the amplitude of the nonadiabatic oscillations increases due to quantum interference.

B. Complete population return

The CPR conditions are given by Eqs. (26) and (27). The former is the condition for single-pulse CPR, which is impossible unless $B=0$ or $A=0$ as discussed. The latter condition originates from quantum interference and can be written down more explicitly as

$$\cosh\tfrac{1}{2}\sqrt{B^2-A^2}\cos\varphi=\cosh\tfrac{1}{2}B\cos\frac{k\pi}{N} \qquad (A<|B|,\ k=1,2,\ldots,N-1)\,, \tag{47a}$$

$$\cos\tfrac{1}{2}\sqrt{A^2-B^2}\cos\varphi=\cosh\tfrac{1}{2}B\cos\frac{k\pi}{N} \qquad (A\geq|B|,\ k=1,2,\ldots,N-1)\,, \tag{47b}$$

from where A can be expressed directly as a function of B because φ does not depend on A. It is easy to see that for any detuning slope B and any number of pulses N Eq. (47a) can always be satisfied by an appropriate choice of the pulse area A and/or the train period T (which is involved in φ), i.e., in the *low-intensity region* ($A<|B|$) CPR is always possible.

Much more interesting is Eq. (47b), which represents the CPR condition in the *high-intensity region* ($A\geq|B|$). Inasmuch as the cases of even and odd number of pulses are quite different we will consider them separately.

Even number of pulses, $N=2n$. Since $\cos(k\pi/N)=0$ for $k=n$, CPR solutions always exist: one group of them is given by $A=[B^2+(2l+1)^2\pi^2]^{1/2}$ ($l=0,1,2,\ldots$) and another by $\varphi(T)=(l+\frac{1}{2})\pi$ ($l=0,1,2,\ldots$). The former condition requires $A^2-B^2\geq\pi^2$ while the latter can be fulfilled by an appropriate choice of T. For other values of k in Eq. (47b), CPR solutions exist as well.

Odd number of pulses, $N=2n+1$. Now $\cos(k\pi/N)\neq0$ for any k and since the LHS of Eq. (47b) is always ≤1 the CPR condition imposes *an upper limit* on $\cosh(\frac{1}{2}B)$, i.e., on B. The weakest restriction is when $|\cos(k\pi/N)|$ is smallest, i.e., when $k=n$. Thus, we find that CPR is possible if

$$|B|\leq\frac{2}{\pi}\ln\left[\cot\frac{\pi}{4N}\right] \qquad (A\geq|B|,\ N=2n+1)\,. \tag{48}$$

Moreover, whenever CPR is possible it occurs for an infinite number of values of the pulse area determined from Eq. (47b).

C. Complete population inversion

The results (25) in Sec. II suggest that in the *low-intensity region* ($A<|B|$) CPI with N Allen-Eberly pulses occurs when both conditions

$$\cosh\tfrac{1}{2}\sqrt{B^2-A^2}\cos\varphi=\cosh\tfrac{1}{2}B\cos\frac{(2k-1)\pi}{2N}\,, \tag{49a}$$

$$\cosh\tfrac{1}{2}\sqrt{B^2-A^2}\sin\varphi=0 \qquad (A<|B|,\ k=1,2,\ldots,N) \tag{49b}$$

are satisfied. Equation (49b) requires $\sin\varphi=0$ and hence $\cos\varphi=\pm1$. After substituting this value into Eq. (49a) one concludes that for any detuning slope B CPI is achieved for n values of A where $N=2n$ or $N=2n+1$.

In the *high-intensity region* ($A\geq|B|$), the CPI conditions have the form

$$\cos\tfrac{1}{2}\sqrt{A^2-B^2}\cos\varphi=\cosh\tfrac{1}{2}B\cos\frac{(2k-1)\pi}{2N} \tag{50a}$$

$$\cos\tfrac{1}{2}\sqrt{A^2-B^2}\sin\varphi=0\,. \qquad (A\geq|B|,\ k=1,2,\ldots,N) \tag{50b}$$

We will consider the cases of even and odd number of pulses separately again.

Odd number of pulses, $N=2n+1$. Since $\cos[(2k-1)\pi/2N]=0$ for $k=n+1$, CPI solutions always exist and one group of them is given by $A=[B^2+(2l+1)^2\pi^2]^{1/2}$ ($l=0,1,2,\ldots$), which suggests that CPI requires $A^2-B^2\geq\pi^2$. The value of φ is unimportant. Another group of CPI solutions is obtained for $\sin\varphi=0$, which is an easily satisfied condition for T. Then $\cos\varphi=\pm1$ in Eq. (50a) and the solutions are determined by solving this equation with respect to A. These additional solutions exist under some restrictions on B similar to Eq. (48).

Even number of pulses, $N=2n$. Now $\cos[(2k-1)\pi/2N]\neq 0$ for any k and the RHS of (50a) is always $\neq 0$. Equation (50b) requires $\sin\varphi=0$; then $\cos\varphi=\pm 1$ in Eq. (50a) and the solutions, if any, are easily determined by solving this equation for A. Since the LHS of Eq. (50a) is always ≤ 1, it is straightforward to show that this equation imposes *an upper limit* on $\cosh(\frac{1}{2}B)$, i.e., on B, for existence of CPI solutions. The weakest restriction is when $|\cos[(2k-1)\pi/2N]|$ is smallest, i.e., when $k=n$ or $k=n+1$. Thus, we obtain that CPI is possible if

$$|B|\leq\frac{2}{\pi}\ln\left[\cot\frac{\pi}{4N}\right]\quad(A>|B|,\ N=2n)\ . \tag{51}$$

Moreover, whenever CPI is possible it occurs for an infinite number of values of the pulse area determined from Eq. (50a).

D. Dependence on the pulse area

In Fig. 10, the transition probability $P_2^{(N)}$ is plotted as a function of the pulse area A for one to ten pulses with $B=4$. The field is assumed to be given by Eq. (4b) with a phase shift $\varphi=0$. It is seen that whenever an odd pulse transfers the population to the excited state in the high-intensity region (on the right from the vertical dotted line) the next even pulse returns it to the ground state and vice versa. CPR is not possible for one, three, and five pulses in the high-intensity region while CPI is not possible for two and four pulses there. For a sufficiently large odd number of pulses CPR becomes possible as does CPI for an even number of pulses. Note that conditions (48) and (51) require $N>5$ for $B=4$. This is explained by the fact that besides adiabatic contributions, the transition probability always contains some nonadiabatic contributions that give rise to oscillations in the populations. Adiabaticity increases when increasing the detuning slope B and consequently, the nonadiabatic contributions and the oscillation amplitude decrease. That is why CPR for a given odd number of pulses as well as CPI for a given even number of pulses are not possible above a certain detuning determined from Eqs. (48) or (51). Increasing the number of pulses for a fixed detuning enhances the effect of nonadiabatic contributions and in fact leads to the same result as decreasing the detuning for a fixed number of pulses: a growing amplitude of oscillations.

We have to note that, as discussed in Sec. II E, the train fields (4a) and (4b) do not lead to qualitatively different results when considering the dependence of $P_2^{(N)}$ on A because the free-evolution phase φ does not depend on A. The same values of $\cos\varphi$, and thus, the same transition probabilities, can be obtained for both Eqs. (4a) and (4b) with appropriately chosen (generally different) train periods T. The dependence of $P_2^{(N)}$ on φ, however, is very substantial. In Fig. 11, the transition probability is plotted against the pulse area for a train of seven pulses with field (4b) for various phase shifts φ. Values of φ from 0 to $\pi/2$ are only shown because $P_2^{(N)}$ is a periodic function of φ with a period of π and because a phase shift of $\pi-\varphi$ gives the same results as a phase shift of φ. An important value is $\varphi=\pi/2$ because then $a_1=0$ [see Eq. (44)] and $\vartheta=\pi/2$ [see Eq. (22)]. As a result, according to Eq. (23b), for N odd, $P_2^{(N)}$ is equal to the single-pulse probability $P_2^{(1)}$ while for N even, $P_2^{(N)}$ is equal to zero irrespective to the detuning slope B, which resembles the case of resonance (Sec. III, Figs. 1 and 2). Another interesting feature seen in Fig. 11 is that in the high-intensity region

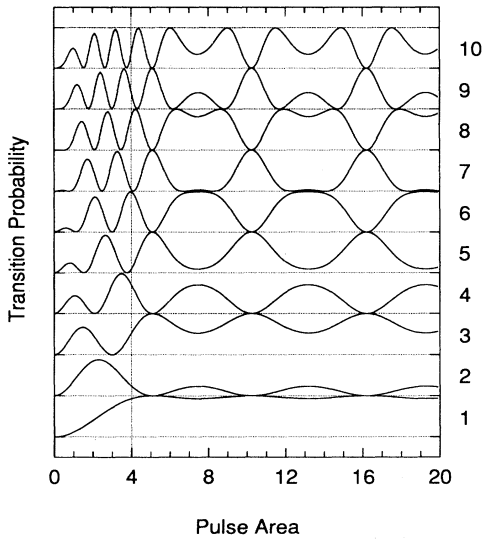

FIG. 10. The transition probability against the pulse area A for a train of one to ten Allen-Eberly pulses (43) (the numbers on the right of the figure) for a detuning slope of $B=4$. The electric field is given by Eq. (4b) and the phase shift is $\varphi=0$. For each curve, the adjacent horizontal dotted lines indicate the values of zero and unity probability. The vertical dotted line separates the low-intensity region (on the left) from the high-intensity region (on the right).

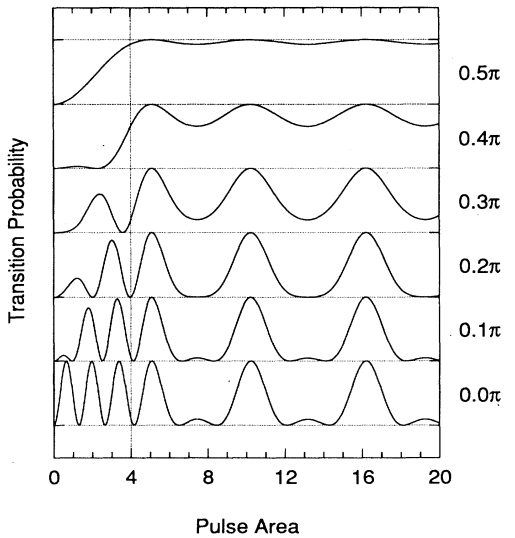

FIG. 11. The transition probability against the pulse area A for a train of seven Allen-Eberly pulses (43) with a detuning slope of $B=4$ for several different values (the numbers on the right of the figure) of the free-evolution phase shift φ between 0 and $\pi/2$. The electric field is given by Eq. (4b). The dotted lines have the same meaning as in Fig. 10.

($A \geq |B|$) CPI occurs at the same values of the pulse area, $A=[B^2+(2l+1)^2\pi^2]^{1/2}$ ($l=0,1,2,\ldots$), regardless of φ, in agreement with the results in Sec. VI C.

E. Dependence on the detuning

In contrast to the rectangular and the Rosen-Zener pulses, the transition probability $P_2^{(N)}$ is an even function of the detuning slope B, both for train (4a) when $\varphi=-\beta\ln[\cosh(T/\tau)]$ and for train (4b) when $\varphi=\frac{1}{2}\omega_a T$, because, as mentioned above, the dependence of $P_2^{(N)}$ on φ [through a_1 (44)] is factorized in $\cos\varphi$ and $P_2^{(N)}$ does not depend on the phase η (45). In Figs. 12(a) and 12(b), the transition probabilities for trains (4a) and (4b) ($T=10\tau$ is assumed for the former and $\varphi=0$ for the latter), respectively, are plotted against the detuning slope B for a pulse area of 3π. We have only shown the high-intensity region ($|B|\leq A$) because it is physically the more interesting one. Outside it, in the low-intensity region, $P_2^{(N)}$ oscillates mainly between zero and one, the number of oscillations being proportional to the number of pulses. The structures in Fig. 12(b) that originate from the $\sin^2(N\vartheta)/\sin^2\vartheta$ factor in $P_2^{(N)}$ (23b) modulate the oscillations in Fig. 12(a). The latter are generated by the factor $\cos\varphi$ in a_1 (44) since in Fig. 12(a), $\varphi=-(B/2\pi)\ln(\cosh T/\tau)$ changes with B in contrast to $\varphi=0$ in Fig. 12(b). The amplitude of the oscillations increases with the number of pulses both in Fig. 12(a) and Fig. 12(b) due to the enhancement of the nonadiabatic effects as discussed in Sec. VI D. This means that any deviation from zero and unity in $P_2^{(1)}$ is greatly enhanced in $P_2^{(N)}$. It is clearly seen that at large detuning the oscilla-

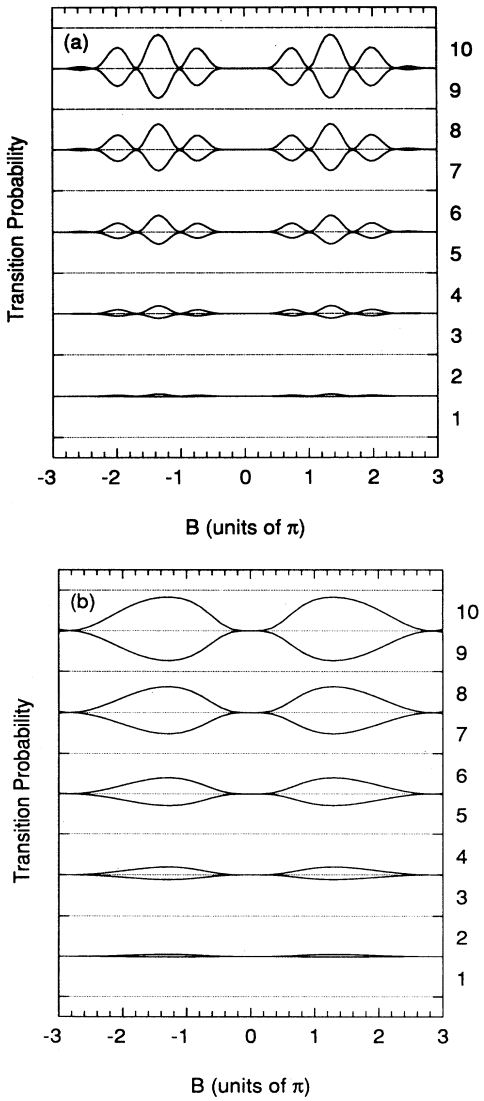

FIG. 12. The transition probability against the detuning slope B for a train of one to ten Allen-Eberly pulses (43) for a pulse area of $A=3\pi$. The dotted lines have the same meaning as in Fig. 10. (a) Field (4a), repetition time $T=10\tau$; (b) field (4b), phase shift $\varphi=0$.

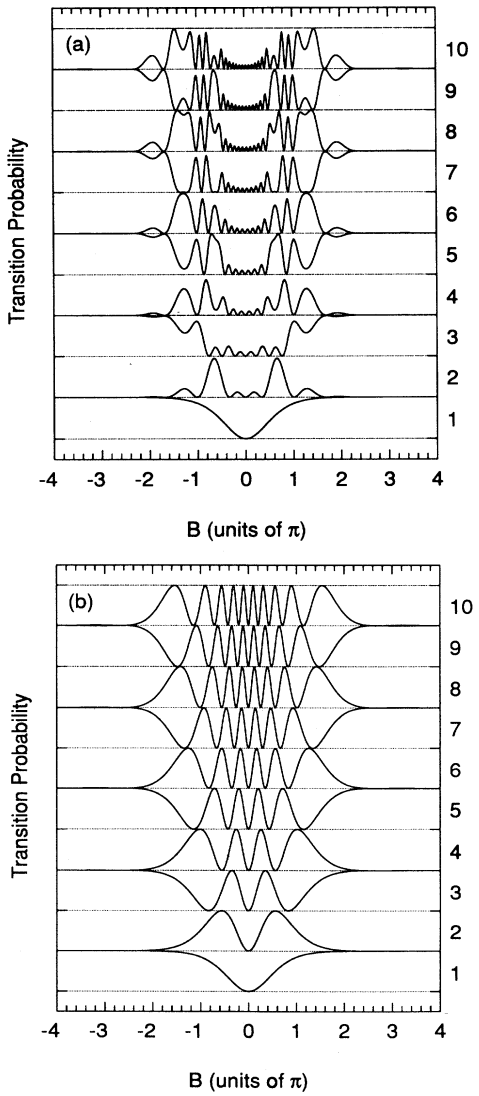

FIG. 13. The same as in Fig. 12 but for a pulse area of $A=4\pi$. (a) Field (4a), repetition time $T=10\tau$; (b) field (4b), phase shift $\varphi=0$.

tions are suppressed because the adiabaticity improves. Furthermore, this suppression gets less effective as the number of pulses increases. At resonance ($B=0$), $P_2^{(N)}$ equals unity for odd N and zero for even N because any consecutive 3π pulse swaps the atomic populations. It should be noted that the absence of oscillations near $B=0$ is not because the excitation is adiabatic but because the single-pulse probability is equal to unity at $B=0$ and to almost unity in some vicinity of this value. Multiple-pulse excitation enhances the nonadiabatic effects only provided the excited-state population is not too close to one or zero.

The situation is markedly different in Figs. 13(a) and 13(b) where the transition probabilities for trains (4a) and (4b), respectively, are plotted against B for a pulse area of 4π at which the transition probability equals zero at resonance ($B=0$) for a single pulse as well as for N pulses. Off resonance, however, the single-pulse probability rises from zero to one as the detuning slope increases and this large change generates oscillations for two and more pulses. The oscillations are more complicated for train (4a) than for train (4b) for the same reasons discussed in connection with Figs. 12(a) and 12(b). The oscillations are damped as the detuning slope B increases, the transitions becoming increasingly adiabatic. Again, this damping gets less effective as the number of pulses increases.

VII. CONCLUSIONS

We have presented a nonperturbative analytical study of coherent excitation of a two-state system by a train of N consecutive equally spaced identical pulses. We have found in a closed form the general relations (21) between the evolution matrix elements in the cases of one and N pulses. Equations (23), which provide the state populations, represent one of the basic results in the paper. They allow us to utilize the available single-pulse analytical solutions in describing pulse-train–induced transitions; for pulses that can only be treated numerically, they shorten the computations by a factor of N. The populations depend on the individual pulse parameters as well as on the repetition time of the train through a phase shift φ accumulated in the course of the free evolution of the system during and between the pulses. The relations show that the multiple-pulse excitation of a two-state system can be considered as a quantum analog of the diffraction grating through the analogy is not absolute. The transition probability reduces to the correct limits in several particular cases studied perturbatively earlier. Simple formulas (25)–(27) are derived for the conditions for complete population inversion and complete population return.

The general results have been applied to four important particular cases: resonant, rectangular, Rosen-Zener, and Allen-Eberly pulses. A general feature in all these cases is that the number and the amplitude of the oscillations in the state populations increase with the number of pulses as a result of quantum interference. The train-induced probability strongly depends on the way the train is produced as the phase shift φ is different. The populations regarded as functions of the detuning Δ show much more complicated features for field (4a), when φ depends on Δ, than for field (4b), when φ does not depend on Δ. On the other hand, regarded as functions of the pulse area A, the populations induced by trains (4a) and (4b) do not differ in principle because φ does not depend on A; the same phase shift can be obtained by appropriate choice of the repetition time T. Because of the phase shift φ, the transition probability in the case of *exact resonance* is not simply given by the single-pulse probability with the single-pulse area A replaced by the total area NA. For *rectangular pulses,* the excitation spectrum has long wings because the single-pulse transition probability, which modulates the pulse-train probability via Eq. (23b), decreases slowly (Lorentzially) versus the detuning. CPI is possible below a given value (36) of the ratio between the detuning and the pulse area. This value increases nearly linearly with the number of pulses. For the *Rosen-Zener pulses* (37), which represent a typical case of excitation by a smooth symmetric pulse with a constant nonzero detuning, CPI becomes possible for a pulse train while it is impossible for a single pulse. Furthermore, there is an upper limit (42) on the detuning for which CPI can be observed. This limit increases logarithmically with the number of pulses. The excitation spectra are much simpler than for the rectangular pulses since the Rosen-Zener pulses are much more adiabatic and the single-pulse transition probability decreases much faster (exponentially) against the detuning. For the *Allen-Eberly pulses* (43) which are chirped, CPR becomes possible for more than one pulses while it is impossible for a single pulse. There are two distinct cases of even and odd number of pulses and two distinct regions of values of the pulse area compared to the detuning slope: the low-intensity (small area) and the high-intensity region (large area). In the low-intensity region, the difference between the odd and the even number of pulses is not very large while in the high-intensity region it is quite pronounced. This is a region where the transitions are mainly adiabatic for large detuning. Any odd pulse transfers the population from the ground state to the excited one while any even pulse returns it to the ground state. As a function of the pulse area, for an odd number of pulses the excited-state population oscillates between one and a nonzero value (for a sufficiently large detuning), the CPI being a typical property. For even number of pulses, the excited-state population oscillates between zero and a value less than one, the typical property being CPR. The amplitude of the oscillations in both cases increases with the number of pulses, which can be explained as due to constructive interference of the nonadiabatic contributions to the populations from the consecutive pulses. In fact, this increase makes CPR possible for large enough odd number of pulses (48) and CPI for large enough even number of pulses (51).

To conclude, we should point out that most of the results obtained in the present paper can be observed experimentally, particularly in view of the recent advances in laser technology, including effective pulse shaping [28] and producing trains of equally spaced identical pulses with repetition times of the order of 10–100 ps [25].

Finally, interesting further generalizations of the re-

sults presented in this work could include nonidentical pulses, relaxation effects, and three-level systems. It is also worth considering trains of asymmetric pulses that show some peculiarities [35] as compared to the symmetric ones.

ACKNOWLEDGMENTS

This work was supported in part by the UK Engineering and Physical Research Council and by the European Union. N.V.V. acknowledges the Royal Society for their financial support.

APPENDIX

We will derive the relations between the elements of the $\mathbf{S}_N$ matrix and the $\mathbf{S}_1$ matrix, which are connected via Eq. (13),

$$\mathbf{S}_N=(\mathbf{S}_1)^N ,$$

by using some basic methods of matrix algebra [36]. Let λ_1 and λ_2 be the eigenvalues of $\mathbf{S}_1$ (11) and $\mathbf{U}$ be the matrix that diagonalizes $\mathbf{S}_1$, i.e.,

$$\mathbf{U}^{-1}\mathbf{S}_1\mathbf{U}=\begin{bmatrix}\lambda_1 & 0\\ 0 & \lambda_2\end{bmatrix}\Longleftrightarrow\mathbf{S}_1=\mathbf{U}\begin{bmatrix}\lambda_1 & 0\\ 0 & \lambda_2\end{bmatrix}\mathbf{U}^{-1} .$$

Then

$$\mathbf{S}_N=(\mathbf{S}_1)^N=\mathbf{U}\begin{bmatrix}\lambda_1^N & 0\\ 0 & \lambda_2^N\end{bmatrix}\mathbf{U}^{-1} .$$

The eigenvalues λ_1 and λ_2 are given by

$$\lambda_1=e^{i\vartheta},\quad \lambda_2=e^{-i\vartheta}$$

where

$$\cos\vartheta=a_1,\quad \sin\vartheta=\sqrt{1-a_1^2} .$$

The matrix $\mathbf{U}$, which can be chosen to be a unitary matrix, i.e., $\mathbf{U}^{-1}=\mathbf{U}^{\dagger}$, is easily constructed from the normalized eigenvectors and is

$$\mathbf{U}=\begin{bmatrix} q & i\dfrac{-b_1+\sqrt{1-a_1^2}}{c_1-id_1}q^* \\ i\dfrac{-b_1+\sqrt{1-a_1^2}}{c_1+id_1}q & q^* \end{bmatrix},$$

where

$$|q|^2=\frac{b_1+\sqrt{1-a_1^2}}{2\sqrt{1-a_1^2}}$$

and the argument of q is of no importance. Then after simple algebra one obtains

$$\mathbf{S}_N=\begin{bmatrix}\cos N\vartheta+ib_1\dfrac{\sin N\vartheta}{\sin\vartheta} & (c_1+id_1)\dfrac{\sin N\vartheta}{\sin\vartheta}\\ (-c_1+id_1)\dfrac{\sin N\vartheta}{\sin\vartheta} & \cos N\vartheta-ib_1\dfrac{\sin N\vartheta}{\sin\vartheta}\end{bmatrix} . \quad \text{(A1)}$$

[1] L. Allen and J. H. Eberly, *Optical Resonance and Two-Level Atoms* (Wiley, New York, 1975).

[2] B. W. Shore, *The Theory of Coherent Atomic Excitation,* Vol. I (Wiley, New York, 1990).

[3] E. E. Nikitin and S. Ya. Umanskii, *Theory of Slow Atomic Collisions* (Springer, Berlin, 1984).

[4] A. E. Kaplan, Zh. Eksp. Teor. Fiz. **65**, 1416 (1973) [Sov. Phys. JETP **38**, 705 (1974)]; *ibid.* **68**, 823 (1975) [**41**, 409 (1975)]; see also V. S. Butylkin, A. E. Kaplan, Yu. G. Khronopulo, and E. I. Yakubovich, *Resonant Nonlinear Interactions of Light with Matter* (Springer, Berlin, 1989), Chap. 3.

[5] N. F. Ramsey, Phys. Rev. **76**, 996 (1949); **78**, 695 (1950); Rev. Mod. Phys. **62**, 541 (1990); *Molecular Beams* (Oxford University Press, New York, 1956).

[6] J. C. Bergquist, S. A. Lee, and J. L. Hall, Phys. Rev. Lett. **38**, 159 (1977).

[7] Ye. V. Baklanov, B. T. Dubetsky, and V. P. Chebotayev, Appl. Phys. **9**, 171 (1976); V. P. Chebotayev, *ibid.* **15**, 219 (1978).

[8] Ye. V. Baklanov, V. P. Chebotayev, and B. Ta. Dubetsky, Appl. Phys. **11**, 201 (1976).

[9] M. M. Salour, Appl. Phys. **15**, 119 (1978); M. M. Salour and C. Cohen-Tannoudji, Phys. Rev. Lett. **38**, 757 (1977).

[10] M. M. Salour, Rev. Mod. Phys. **50**, 667 (1978).

[11] T. W. Hänsch, in *Tunable Lasers and Applications,* edited by A. Mooradian, T. Jaeger, and P. Stoksєh (Springer, Berlin, 1976), Vol. III, p. 326; R. Teets, J. Eckstein, and T. W. Hänsch, Phys. Rev. Lett. **38**, 760 (1977); J. N. Eckstein, A. I. Ferguson, and T. W. Hänsch, *ibid.* **40**, 847 (1978).

[12] J. Mlynek, W. Lange, H. Harde, and H. Burggraf, Phys. Rev. A **24**, 1099 (1981); B. Cagnac, Philos. Trans. R. Soc. London A **307**, 633 (1982); N. F. Scherer *et al.*, *ibid.* **93**, 856 (1990); N. F. Scherer *et al.*, J. Chem. Phys. **95**, 1487 (1991); E. Marega, V. S. Bagnato, and S. C. Zilio, Opt. Lett. **18**, 1751 (1993).

[13] G. F. Thomas, Phys. Rev. A **35**, 5060 (1987).

[14] R. J. Temkin, J. Opt. Soc. Am. B **10**, 830 (1993).

[15] E. Krüger, Z. Phys. D **31**, 13 (1994); J. Opt. Soc. Am. B **12**, 15 (1995).

[16] P. W. Milonni and L. E. Thode, Appl. Opt. **31**, 785 (1992).

[17] L. C. Bradley, J. Opt. Soc. Am. B **9**, 1931 (1992).

[18] A. Gavrielides and P. Peterson, Opt. Commun. **104**, 46 (1994).

[19] P. Peterson and A. Gavrielides, Opt. Commun. **104**, 53 (1994).

[20] M. A. Newbold and G. J. Salamo, Phys. Rev. A **22**, 2098 (1980).

[21] P. L. Knight and P. E. Coleman, J. Phys. B **13**, 4345 (1980); P. E. Coleman, D. Kagan, and P. L. Knight, Opt. Commun. **36**, 127 (1981); B. J. Dalton, T. D. Kieu, and P. L. Knight, Opt. Acta **33**, 459 (1986).

[22] J. E. Thomas, P. R. Hemmer, S. Ezekiel, C. C. Leiby, Jr., R. H. Picard, and C. R. Willis, Phys. Rev. Lett. **48**, 867 (1982).

[23] P. T. Greenland, J. Phys. B **16**, 2515 (1983).

[24] G. F. Thomas, Phys. Rev. A **41**, 1645 (1990).

[25] O. Saether, B. E. Flaten, and O. Aaserud, Electron. Lett. **27**, 1227 (1991); E. J. Beiting, Appl. Opt. **31**, 2642 (1992);

E. Yamada, K. Wakita, and M. Nakazawa, Electron. Lett. **29**, 845 (1993); S. V. Chernikov, J. R. Taylor, and R. Kashyap, *ibid.* **29**, 1788 (1993); Opt. Lett. **19**, 539 (1994).

[26] Y. S. Bai, A. G. Yodh, and T. W. Mossberg, Phys. Rev. Lett. **55**, 1277 (1985).

[27] B. Broers, H. B. van Linden van den Heuvell, and L. D. Noordam, Phys. Rev. Lett. **69**, 2062 (1992); D. Goswami and W. S. Warren, J. Chem. Phys. **101**, 6439 (1994).

[28] C. W. Hillegas, J. X. Tull, D. Goswami, D. Strickland, and W. S. Warren, Opt. Lett. **19**, 737 (1994); W. S. Warren, in *Atomic and Molecular Processes with Short Intense Laser Pulses,* edited by A.D. Bandrauk, NATO ASI Ser. B, Vol. 171 (Plenum, New York, 1988), p. 1.

[29] N. Rosen and C. Zener, Phys. Rev. **40**, 502 (1932).

[30] Yu. N. Demkov and M. Kunike, Vestn. Leningr. Univ. Fis. Khim. **16**, 39 (1969) (in Russian); see also K.-A. Suominen and B. M. Garraway, Phys. Rev. A **45**, 374 (1992).

[31] F. T. Hioe, Phys. Rev. A **30**, 2100 (1984); F. T. Hioe and C. E. Carroll, *ibid.* **32**, 1541 (1985).

[32] Yu. A. Brychkov, O. I. Marichev, and A. P. Prudnikov, *Tables of Indefinite Integrals* (Nauka, Moscow, 1986) (in Russian); The formulas can also be obtained by transformation of relations 1.331 and1.332 of I. S. Gradshteyn and I. M. Rizhik, *Table of Integrals, Series and Products* (Academic, New York, 1980).

[33] I. I. Rabi, Phys. Rev. **51**, 652 (1937).

[34] L. D. Landau, Phys. Z. Sowjetunion **2**, 46 (1932); C. Zener, Proc. R. Soc. London A **137**, 696 (1932); E. C. G. Stueckelberg, Helv. Phys. Acta **5**, 369 (1932).

[35] A. Bambini and P. R. Berman, Phys. Rev. A **23**, 2496 (1981); C. E. Carroll and F. T. Hioe, *ibid.* **41**, 2835 (1990); N. V. Vitanov, J. Phys. B **27**, 1351 (1994); *ibid.* **28**, L19 (1995); N. V. Vitanov and P. L. Knight, *ibid.* **28**, 1905 (1995).

[36] M. C. Pease III, *Methods of Matrix Algebra* (Academic, New York, 1965).